Journal of the Mechanical Behavior of Biomedical Materials 170 (2025) 107106

Contents lists available at ScienceDirect

Journal of the Mechanical Behavior of Biomedical Materials

journal homepage: www.elsevier.com/locate/jmbbm

Impact of polishing, glazing and firing, restoration thickness, point of loading and aging on the edge chipping resistance of lithium silicate ceramics

Carola Irlinger *, Bogna Stawarczyk, John Meinen, Daniel Edelhoff, Felicitas Mayinger

Department of Prosthetic Dentistry, University Hospital, LMU Munich, Goethestraße 70, 80336, Munich, Germany

ARTICLE INFO

Keywords:
Edge chipping resistance
Silicate ceramics
CAD/CAM milling
Restoration thickness
Surface treatment
Artificial aging

ABSTRACT

Objectives: To investigate the edge chipping resistance (ECR) of four lithium silicate ceramics at different thicknesses and points of loading after various surface treatment, firing and aging protocols.
Methods: 288 rectangular specimens were cut from CAD/CAM ceramics (lithium-di-silicate: Amber Mill, Amber Mill Direct, IPS e.max CAD; lithium-alumino-silicate: CEREC Tessera) in three thicknesses (1.5 mm, 2 mm, 3 mm) and underwent different surface treatments (polishing, glazing, no surface treatment) and/or firing protocols (high translucency, medium opacity). Specimens were bonded to 4 mm thick dentine analogues and loaded 0.25 mm or 0.30 mm from the edge using a Vickers diamond indenter. ECR was determined initially, after thermocycling (5/55 °C, 10,000 cycles) and after hydrothermal aging (134 °C, 0.2 MPa, 120min). Force when chipping occurred was recorded and ECR calculated. Data were analyzed with Kolmogorov-Smirnov, Kruskal-Wallis, Mann-Whitney U, Friedmann and Wilcoxon tests ($p < 0.05$).
Results: For 7/18 groups, glazed and medium opacity fired Amber Mill showed higher ECR than all other groups. In comparison with polishing or exclusive firing, a surface treatment with glazing led to the highest ECR. The influence of specimen thickness and point of loading was negligible. While aging reduced the ECR in 50 % of the glazed groups, the ECR of those groups remained among the highest.
Significance: With the majority of groups showing no impact of the specimen thickness, a reduced restoration thickness of 1.5 mm seems to present limited disadvantages and should thus be considered for minimal invasive treatments. With regards to ECR, glazing can be recommended as the preferred surface treatment method for CAD/CAM lithium silicate ceramics.

1. Introduction

Dental restorations made of monolithic lithium silicate ceramics present an array of favorable properties, such as appealing esthetics, favorable wear behavior, chemical resistance, as well as high biocompatibility (Anusavice, 1992). Indications for all-ceramic lithium silicate restorations are broad, including monolithic crowns, bridges up to the second premolar, inlays and onlays as well as veneers (Zhang and Kelly, 2017). Lithium silicate ceramics can be subclassified as lithium-di-silicate, lithium-meta-silicate, lithium-alumina-silicate and lithium-di/alumina-silicate due to differences in the chemical composition, microstructure, crystallinity and mechanical properties (Stawarczyk et al., 2021). A crystalline phase containing high proportions of lithium-meta-silicate crystals is mainly found in pre-crystallized materials and is associated with a reduced fracture toughness, yet better machinability (Lohbauer et al., 2024). Glass-ceramics containing lithium-alumina-silicate exhibit a low thermal expansion coefficient, as well as a high thermal impact resistance and translucency due to their grain size being smaller than the wavelength of visible light (Li et al., 2023). So-called advanced lithium-di-silicate ceramics (ALD), containing lithium-di-silicate and lithium-alumina-silicate crystals, are reported to possess a higher wear resistance in the material itself and towards antagonistic tooth structures, as well as a lower surface roughness, yet lower fatigue failure compared to conventional lithium-di-silicate ceramics (Rosentritt et al., 2022; Freitas et al., 2023).

In the digital workflow, lithium silicate ceramics are milled from CAD/CAM blocks. The use of diamond grinding tools during CAD/CAM

* Corresponding author.
E-mail address: carola.irlinger@med.uni-muenchen.de (C. Irlinger).

https://doi.org/10.1016/j.jmbbm.2025.107106
Received 25 April 2025; Received in revised form 10 June 2025; Accepted 19 June 2025
Available online 20 June 2025

machining can effectuate surface damages in the material and cause an increased surface roughness, which can lead to an increased fatigue property, resulting in the chipping or fracture of the restoration (Alao et al., 2021; Coldea et al., 2015). Local structural defects act as starting points for microcrack formation, making it possible for liquids to penetrate and cause the formation and propagation of cracks (Chen et al., 1999). Due to the ceramics' brittleness and their low ability to withstand tension, stress applied to said area can lead to the immediate formation of cracks without prior plastic deformation. The ceramic material, compromised in its flexural strength by the cracks, tends to rapidly propagate cracks even under loads that are significantly below the actual flexural strength of the material and therefore is prone to fracture and failure (Joshi et al., 2014). This aspect is notable for thin restoration margins, both during milling, try-in, insertion and clinical usage of the restoration. Therefore, the ability of a ceramic to resist crack initiation and propagation plays a significant role in the occurrence of chippings that can result in reduced esthetics, discolorations or, in the worst case, the failure of the entire restoration (Zhang et al., 2009; Quinn et al., 2014; Mores et al., 2017). For this reason, optimal surface treatments are essential to produce an even surface, increase the material's flexural strength and hence reduce the fracture probability (Chen et al., 1999; de Jager et al., 2000).

Depending on the product, lithium silicate restorations are milled in a pre-crystalized or fully crystalized state and subsequently processed by exclusively polishing the restoration or undergoing a crystallization firing, a process that can be paired with glazing. In this context, a surface treatment with polishing is supposed to reduce the depth of preexisting cracks and produce a smooth surface free of porosities (Asai et al., 2010). The same goal is pursued during crystallization firing, which previous studies have shown to induce "healing" of cracks generated by CAM grinding (Denry, 2013; Fairhurst et al., 1992; Lu et al., 2023). This processing step can be performed using different firing protocols provided by the respective manufacturer. For Amber Mill, two firing protocols exist that allow freedoms in the esthetic design of the restoration by supposedly resulting in high translucency or medium opacity. In the process of glazing, the restoration is strengthened by the penetration of the glazing compound into defects or cracks, thus reducing the depth of surface inhomogeneities (de Jager et al., 2000; Fairhurst et al., 1992). In addition, compressive stress within the ceramic can be generated through the application of glazing material, with possesses a lower coefficient of thermal expansion than the ceramic, which counteracts the formation and propagation of cracks and increases the material's strength (Salmang and Scholze, 2007).

In the following, it is investigated how different treatment protocols, such as polishing, the application of glazing material and subsequent firing, exclusive firing or different firing parameters as well as artificial aging affect the edge chipping resistance (ECR) of four different lithium silicate ceramics, three of which being lithium disilicate ceramics (Amber Mill, Amber Mill Direct and IPS e.max CAD) and one lithium alumina silicate ceramic (CEREC Tessera). The null hypotheses were that different lithium silicate ceramics, different treatment protocols, specimen thicknesses, measuring distances and aging protocols would not influence the ECR.

2. Material & methods

Rectangular-shaped specimens (N = 288) measuring 12 × 14mm with a thickness of 1.5 mm, 2 mm and 3 mm were cut (Secotom-50; Struers, Ballerup, Denmark) from CAD-CAM blocks of 4 different materials (Table 1, Fig. 1) by using a diamond cutting disc (Diamond Cut-off Wheel M1D13; Struers) under water cooling at a rotation speed of 3300U/min and a feed speed of 0.03 mm/s. All specimens were polished

Table 1
– Materials, lot numbers (LOT-#), abbreviations (Abbr.), subgroups, manufacturers, compositions, treatments, types of ovens and firing parameters.

	Material & LOT-#	Treatment	Abbr.	Manufacturer	Composition (in % by weight)	Oven	Firing parameters
Lithium-di-silicate	Amber Mill (AM) EBE06OH0902	Glazing (IPS e.max CAD Crystall./Glaze Spray) and firing for high translucency	AM-G&HTF	Hass Bio, Gangneung-si, South Korea	SiO_2: >65.0Li_2O: >10.0Other oxides and colorants: <25.0	Ivoclar Programat EP 5010	Closing time: 03:00 minTemperature increase rate: 60 °C/minHolding temperature: 815 °CHolding time: 15:00 min
		Glazing (IPS e.max CAD Crystall./Glaze Spray) and firing for medium opacity	AM-G&MOF			Ivoclar Programat EP 5010	Closing time: 03:00 minTemperature increase rate: 60 °C/minHolding temperature: 860 °CHolding time: 15:00 min
	Amber Mill Direct (AD) JBE06OF2001	Polishing	AD-Pol	Hass Bio, Gangneung-si, South Korea	SiO_2: >65.0Li_2O: >10.0Other oxides and colorants: <25.0	–	–
		Glazing (IPS e.max CAD Crystall./Glaze Spray) and firing	AD-G&F			Ivoclar Programat EP 5010	Closing time: 03:00 minTemperature increase rate: 45 °C/minHolding temperature: 815 °CHolding time: 01:00 min
		Firing	AD-F				
Lithium-alumina-silicate	CEREC Tessera (CT)16015174	Glazing (Dentsply Sirona Universal Spray Glaze Fluo) and firing	CT-G&F	Dentsply Sirona, Konstanz, Germany	SiO_2: 55.0–70.0 LiO_2: 5.0–20.0 ZrO_2: 3.0–20.0 Other oxides: 0.0–30.0	Dekema Austromat 654 press-i-dent	Closing time: 01:00 minTemperature increase rate: 55 °C/minHolding temperature: 750 °CHolding time: 02:00 min
		Firing	CT-F			Dekema Austromat 654 press-i-dent	Closing time: 01:00 minTemperature increase rate: 55 °C/minHolding temperature: 750 °CHolding time: 02:00 min
Lithium-di-silicate	IPS e.max CAD (EC)YB54FX	Glazing (IPS e.max CAD Crystall./Glaze Spray) and firing	EC-G&F	Ivoclar, Schaan, Liechtenstein	SiO_2 57.0–80.0; Li_2O 11.0–19.0 K_2O 0.0–13.0; P_2O_5 0.0–11.0 ZrO_2 0.0–8.0; ZnO 0.0–8.0 Al_2O_3 0.0–5.0; MgO 0.0–5.0 Coloring oxides 0.0–8.0	Ivoclar Programat EP 5010	Closing time: 06:00 minTemperature increase rate 1: 90 °C/minHolding temperature 1: 830 °CHolding time 1: 00:10 minTemperature increase rate 2: 30 °C/minHolding temperature 2: 850 °CHolding time 2: 07:00 min

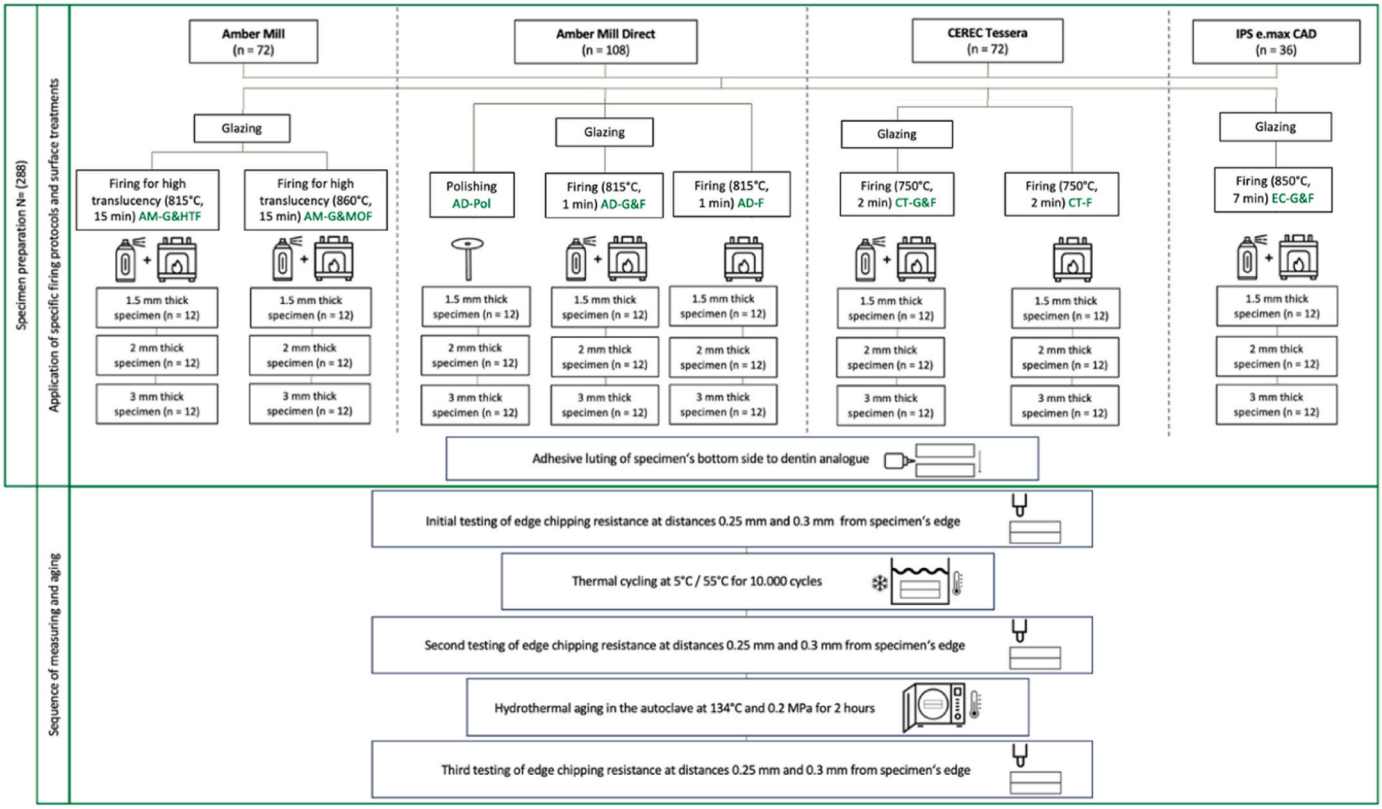

Fig. 1. Study design.

(Abramin; Struers) under water cooling using P500-grit silicon carbide paper (SiC Paper #500, Struers). Thereafter, specimens were cleaned in distilled water for 3 min in an ultrasonic bath (L&R Transistor Ultrasonic T-14; L&R, New Jersey, USA). Specimens underwent different surface treatments and firing protocols.

Amber Mill (Hass Bio, Gangneung-si, South Korea) (AM) specimens were coated with glazing spray (IPS e.max CAD Crystall./Glaze Spray, Ivoclar, Schaan, Liechtenstein) and crystallized according to the manufacturer's instructions (Austromat 654 press-i-dent, Dekema, Freilassing, Germany). For one group of AM specimens, the firing protocol for the translucency grade "high translucency" was applied (hereafter referred to as AM-G&HTF), while the other group received firing following the firing protocol for the translucency grade "medium opacity" (AM-G&MOF).

Amber Mill Direct (Hass Bio) (AD) specimens were divided into three groups: specimens of the first group were polished by hand using diamond polishing wheels (Diapro R17DPmf, Diapro R17DP; EVE Ernst Vetter, Keltern, Germany) (AD polished). Specimens of the second group were glazed (IPS e.max CAD Crystall./Glaze Spray) and subsequently fired (Austromat 654 press-i-dent) (AD-G&F). Specimens belonging to the third group were solely fired (Austromat 654 press-i-dent) (AD-F).

Specimens made of CEREC Tessera (Dentsply Sirona, Hanau, Germany) (TE) were either glazed (Universal Spray Glaze Fluo, Dentsply Sirona, Konstanz, Germany) and fired (CT-G&F) or soley fired (Austromat 654 press-i-dent) (CT-F).

EC Specimens were all glazed (IPS e.max CAD Crystall./Glaze Spray) and fired (Austromat 654 press-i-dent) (EC-G&F).

Silicate ceramic specimens were bonded to dentine analogues with a thickness of 4 mm. Analogues were fabricated from GrandioSO x-tra (Cuxhaven, Germany) using negative molds. The bonding surface of the dentine analogue was airborne-particle abraded with 50 μm alumina (Aluminiumoxid-Edelkorund, Orbis Dental Handelsgesellschaft, Münster, Germany) for 10 s. Afterwards the dentin analogues were cleaned in distilled water in an ultrasonic bath (L&R Transistor Ultrasonic T-14) and left to dry. Monobond Plus (Ivoclar) was applied to the surface using a microbrush and left to dry for 60 s. The bonding surface of the ceramic platelets was treated with 9 % hydrofluoric acid (Porcelain Etch, Ultradent, Brunnthal, Germany) for 20 s, then cleaned by rinsing with water and dried before Monobond Plus (Ivoclar) was applied with a microbrush. A dual-curing luting resin composite (Variolink Esthetic DC, Ivoclar) was used to connect the two components. Excess luting resin composite was removed before light curing was performed for 10 s from each side (D-Light Pro, GC International, Luzern, Switzerland). The bonded specimens were then stored in water at 37 °C in an incubator (HERAcell 150, Heraeus Precious Metals, Hanau, Germany) for 24 h.

The ECR was measured (ZHU 0,2; Zwick Roell) (Figs. 2 and 3) initially, after thermocycling and after hydrothermal aging. 12 measurements at 0.25 mm and 0.3 mm from the edge were performed for each subgroup at each aging level. To determine the maximum loading force at which chipping occurs, specimens were firmly clamped in a vice and subjected to force. The precise location of the applied force and distance from the edge were verified for each specimen employing an integrated optical unit with a measuring microscope (magnification x5, camera resolution: 1.4 megapixels) and the line measurement function (testX-pert V12.3 Master; Zwick). The force was applied through a Vickers diamond indenter ($\alpha = 136°$) positioned with the diagonals of the pyramid aligned to the edge of the specimen at a rate of 10 mm/min until chipping occurred. The maximum force was regarded as the chipping force referred to as F_{max}. The edge chipping resistance was calculated by dividing the maximum applied force by the distance to the edge from the center of the applied force.

For the first aging cycle, specimens were thermocycled in a 5/55 °C distilled water bath for 10,000 cycles (Thermocycler TCS-10; SD Mechatronik, Feldkirchen-Westerham, Germany) with a dwell time set at 20 s. The number of 10,000 cycles is reported to represent approximately one year in vivo (Gale and Darvell, 1999).

For the second aging cycle, the specimens were subjected to

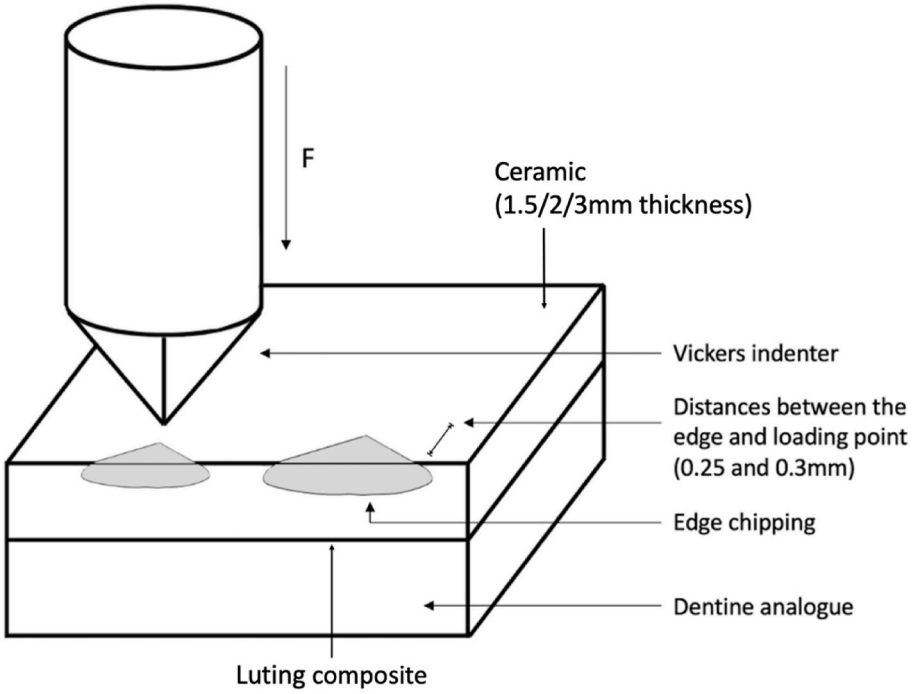

Fig. 2. Set-up for the edge chipping resistance measurement, showing the two distances between the edge and loading point.

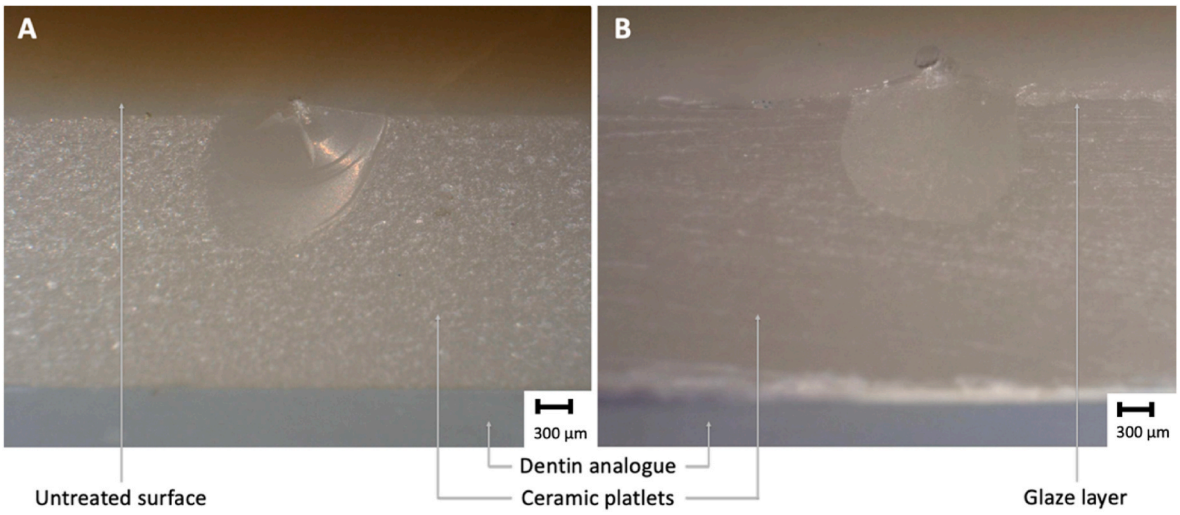

Fig. 3. Digital microscopy images of specimens belonging to different material and treatment groups. (A) Lateral surface of a fired CEREC Tessera specimen. (B) Lateral surface of a glazed IPS e.max CAD specimen.

hydrothermal aging (Euroklav 29-S; MELAG Medizintechnik, Berlin, Germany) at 134 °C for a total of 2 h at a water vapor pressure of 0.2 MPa, corresponding to roughly 6 years in vivo (Deville et al., 2006).

Fracture assessment of the chipping patterns was conducted by using a digital light microscope (VHX-970f, Keyence, Osaka, Japan) at 20-2000× magnification (Zadeh et al., 2021).

Data were descriptively analyzed. The Kolmogorov–Smirnov test was used to test for a violation of the normal distribution (38 of 143 of groups showed a deviation from the normal distribution). Therefore, the effect of the different variables on the ECR was examined with Kruskal-Wallis and Mann-Whitney U tests. The impact of aging was analyzed by Friedmann and Wilcoxon tests. P-values below 0.05 were regarded as statistically significant (IBM Statistics SPSS 29.0, IBM, Amonk, USA).

3. Results

3.1. Impact of the material and treatment on ECR

Within the **1.5 mm thick** non-aged group and 0.25 mm distance, AM-G&HTF, AM-G&MOF, AD-G&F and EC-G&F showed higher ECR ($p < 0.001$) (Table 2, Fig. 4). Within 0.3 mm distance, AM-G&MOF had higher values than AM-G&HTF ($p = 0.002$). AM-G&HTF, AM-G&MOF and EC-G&F showed higher ECR than all AD groups, as well as CT-F ($p = 0.001–0.034$). Within thermal-aged group and 0.25 mm distance, values for AD-Pol, AD-F, CT-G&F and CT-F were lower than all other groups ($p < 0.001–0.041$). AM-G&MOF exhibited the highest ECR, followed by AM-G&HTF ($p = 0.025$). Within 0.3 mm distance, AM-G&MOF and EC-G&F showed higher ECR ($p < 0.001–0.037$). Within hydrothermal-aged group and 0.25 mm distance, AD-Pol, AD-G&F, AD-F, CT-G&F and CT-F,

Table 2
Descriptive statistics (Minimum (Min), Median (Med), Maximum (Max)) for ECR (N/mm) of the different groups.

Material	Treatment	Thickness [mm]	Distance [mm]	No aging	Thermal aging	Hydrothermal aging
				ECR Min/Med/Max (N/mm)	ECR Min/Med/Max (N/mm)	ECR Min/Med/Max (N/mm)
Amber Mill	Glazed & HT-Fired (AM-G&HTF)	1.5	0.25	262/369/803$^{*zB\alpha cd}$	261/287/801$^{*zB\alpha c}$	217/279/372$^{zA\alpha b}$
			0.3	269/318/387$^{zA\beta bc}$	219/278/315$^{zA\beta c}$	180/230/336$^{zA\alpha a}$
		2	0.25	229/297/376$^{zAB\beta c}$	245/312/801$^{*yB\beta de}$	219/286/354$^{zA\alpha cd}$
			0.3	223/301/358$^{zA\alpha d}$	210/250/341$^{zA\alpha c}$	229/256/305$^{zA\alpha d}$
		3	0.25	149/246/800$^{*zA\alpha ce}$	175/209/635$^{*zA\alpha abcd}$	199/282/362$^{zA\alpha e}$
			0.3	200/330/668$^{*zA\alpha d}$	229/295/384$^{yA\alpha c}$	229/265/462$^{*zA\alpha df}$
	Glazed & MO-Fired (AM-G&MOF)	1.5	0.25	365/416/802$^{*zA\gamma d}$	313/375/461$^{zA\beta d}$	237/293/385$^{zA\alpha b}$
			0.3	316/387/668$^{zA\beta d}$	181/342/604$^{*zA\alpha\beta e}$	269/303/421$^{zA\alpha b}$
		2	0.25	335/386/801$^{*zA\beta d}$	265/342/629$^{*zA\alpha e}$	233/316/507$^{zA\alpha\beta d}$
			0.3	301/403/669$^{zA\alpha e}$	303/370/609$^{zA\alpha d}$	218/318/405$^{zA\alpha e}$
		3	0.25	199/372/803$^{*zA\alpha f}$	302/365/460$^{yA\alpha e}$	215/332/403$^{zA\alpha f}$
			0.3	281/593/668$^{*zA\beta e}$	223/342/446$^{zA\alpha c}$	281/320/415$^{zA\alpha ef}$
Amber Mill Direct	Polished (AD-Pol)	1.5	0.25	153/180/293$^{zA\alpha ab}$	151/166/181$^{zA\alpha a}$	143/167/194$^{zA\alpha a}$
			0.3	130/144/259^{zAa}	136/183/199^{zAae}	182^{zAab}
		2	0.25	155/233/806$^{*zA\alpha ab}$	124/206/339$^{zA\alpha abc}$	153/200/232$^{zA\alpha a}$
			0.3	154/225/266$^{zA\alpha ac}$	152/195/237$^{zA\alpha a}$	162/187/215$^{zA\alpha a}$
		3	0.25	156/217/445$^{*zA\alpha bc}$	139/208/286$^{zA\alpha ac}$	146/202/596$^{*zA\alpha bc}$
			0.3	176/243/316$^{zA\alpha b}$	172/215/258$^{zA\alpha a}$	153/207/254$^{zA\alpha a}$
	Glazed & Fired (AD-G&F)	1.5	0.25	220/339/806$^{*yB\gamma c}$	196/245/353$^{zB\beta b}$	145/181/301$^{zA\alpha a}$
			0.3	167/213/287$^{zA\alpha a}$	185/222/270$^{zA\alpha b}$	171/206/300$^{*zA\alpha a}$
		2	0.25	158/223/364$^{zA\alpha a}$	156/194/233$^{zA\alpha a}$	159/182/367$^{*zA\alpha a}$
			0.3	190/280/372$^{yB\beta bcd}$	123/228/291$^{zA\alpha ab}$	130/197/215$^{zA\alpha ab}$
		3	0.25	239/320/802$^{*zB\beta def}$	199/270/327$^{zB\alpha bcd}$	193/245/286$^{zB\alpha cd}$
			0.3	181/292/463$^{zB\beta c}$	224/254/313$^{zB\beta b}$	206/227/265$^{zB\alpha bc}$
Amber Mill Direct	Fired (AD-F)	1.5	0.25	177/226/240$^{zA\alpha b}$	141/174/197$^{zA\alpha a}$	166/168/189$^{zA\alpha a}$
			0.3	222/224/226^{zAa}	204^{zAabcde}	204^{zAab}
		2	0.25	153/286/806$^{*zB\alpha bc}$	154/209/285$^{zB\alpha ab}$	134/181/357$^{zA\alpha a}$
			0.3	203/214/667$^{*zA\alpha abc}$	166/180/285$^{*zA\alpha a}$	169/201/241$^{zA\alpha ab}$
		3	0.25	139/214/801$^{*zA\alpha abc}$	150/207/275$^{zB\alpha ac}$	141/160/233$^{*zA\alpha a}$
			0.3	140/214/218$^{zA\beta ab}$	159/204/241$^{zA\alpha\beta a}$	127/175/318$^{*zA\alpha a}$
CEREC Tessera	Glazed & Fired (CT-G&F)	1.5	0.25	185/213/246$^{zA\alpha b}$	153/189/215$^{zA\alpha a}$	172/188/204$^{zA\alpha a}$
			0.3	213/240/268^{zAac}	146/197/198^{*zAabe}	161/185/208^{zAa}
		2	0.25	178/223/304$^{zA\alpha a}$	200/227/265$^{zB\alpha bc}$	195/255/318$^{zA\alpha b}$
			0.3	177/196/277$^{zA\alpha a}$	155/210/249$^{zA\alpha a}$	192/224/287$^{zAB\alpha c}$
		3	0.25	148/203/265$^{zA\alpha ab}$	159/272/386$^{zB\alpha\beta cd}$	226/259/325$^{zA\beta de}$
			0.3	195/219/296$^{zA\alpha b}$	214/246/284$^{zB\alpha b}$	202/246/305$^{zB\alpha cd}$
	Fired (CT-F)	1.5	0.25	138/184/235$^{zA\alpha a}$	127/175/226$^{zA\alpha a}$	128/148/175$^{zA\alpha a}$
			0.3	145/170/195^{zABa}	143/144/177^{*zAa}	–
		2	0.25	138/197/801$^{*zA\alpha ab}$	154/189/253$^{zA\alpha a}$	145/191/244$^{zB\alpha a}$
			0.3	152/295/669$^{*zB\alpha cd}$	156/183/280$^{zAB\alpha a}$	195/210/228$^{zA\alpha bc}$
		3	0.25	142/174/249$^{zA\alpha a}$	138/196/262$^{zA\alpha a}$	133/188/262$^{zB\alpha ab}$
			0.3	146/190/235$^{zA\alpha a}$	181/214/300$^{zB\alpha a}$	170/195/251$^{*zA\alpha ab}$
IPS e.max CAD	Glazed & Fired (EC-G&F)	1.5	0.25	269/399/802$^{*zA\beta cd}$	231/257/392$^{*zA\alpha b}$	218/273/418$^{zA\alpha\beta b}$
			0.3	249/325/667$^{zA\alpha cd}$	276/335/376$^{yB\alpha de}$	189/257/326$^{zA\alpha a}$
		2	0.25	257/312/803$^{*zA\alpha c}$	171/255/460$^{zA\alpha c}$	167/261/370$^{zA\alpha bc}$
			0.3	256/350/670$^{zA\beta e}$	178/241/334$^{zA\alpha bc}$	196/232/355$^{*zA\alpha cd}$
		3	0.25	214/364/802$^{*zA\beta ef}$	145/281/351$^{zA\alpha d}$	194/222/327$^{*zA\alpha cde}$
			0.3	238/436/529$^{*zA\beta d}$	227/343/450$^{yB\alpha c}$	180/353/495$^{yB\alpha f}$

* Deviation from the normal distribution.
^{zy} Indicate significant differences between **distances** within one aging level, treatment and thickness level.
^{ABC} Indicate significant differences between **thicknesses** within one aging level, treatment and distance level.
$^{\alpha\beta\gamma}$ Indicate significant differences between **agings** within one Distance level, thickness level and treatment.
^{abcdef} Indicate significant differences between **treatments** within one aging level, thickness and distance level.

showed lower ECR than AM-G&MOF, AM-G&HTF and EC-G&F ($p = 0.001–0.034$). Within 0.3 mm distance, AM-G&MOF exhibited the highest ECR ($p < 0.001–0.045$).

Within the treatment "CT-F″, overchipping occurred in all measurements (Fig. 5). The chip extended through the entire thickness of the ceramic layer. Adhesive fractures between the dentin analog and the luting composite were observed, leaving the dentin analog underneath undamaged. Wallner lines, rib shaped marks running perpendicular to the direction of the crack propagation, and hackle marks, spreading within the ceramic parallel to crack propagation direction, were identified.

Within the **2 mm thick** non-aged group and 0.25 mm distance AM-G&MOF had the highest overall ECR, followed by AM-G&HTF and EC-G&F ($p=<0.001–0.022$) (Fig. 6). Within 0.3 mm distance, AM-G&MOF and EC-G&F showed the highest ECR compared to all other treatment groups ($p < 0.001–0.026$). Within thermal-aged groups and 0.25 mm distance, AM-G&HTF and AM-G&MOF showed the highest ECR ($p = 0.016–0.033$). Within 0.3 mm distance AM-G&MOF showed the highest ECR ($p < 0.001$). Within hydrothermal-aged group and 0.3 mm distance, compared to AM-G&HTF, AM-G&MOF showed higher ECR ($p = 0.01$) and also had the overall highest ECR compared to all other groups ($p < 0.001–0.015$).

Within the **3 mm thick** non-aged group and 0.25 mm distance AM-G&MOF had higher ECR than AM-G&HTF ($p = 0.017$) (Fig. 7). Within 0.3 mm distance, AD-Pol, AD-F, CT-G&F and CT-F showed lower ECR than all other treatment groups ($p < 0.001–0.011$). AM-G&MOF presented the highest ECR ($p = 0.011–0.039$). Within the thermal-aged group and 0.25 mm distance, AM-G&MOF showed the overall highest

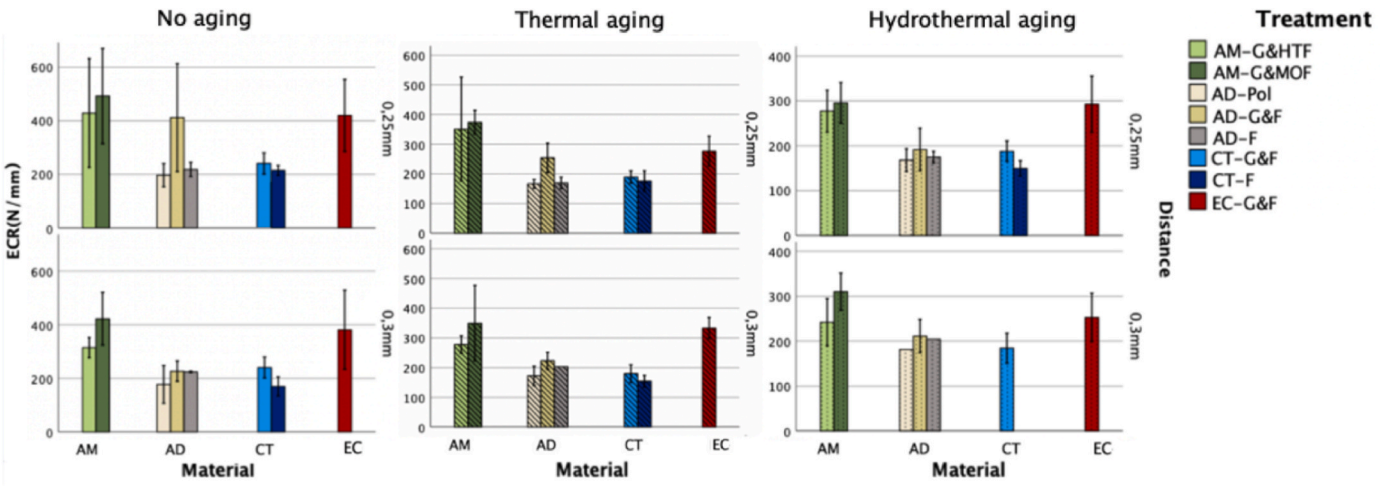

Fig. 4. Edge Chipping results for the four differently treated materials at **1.5 mm** thickness.

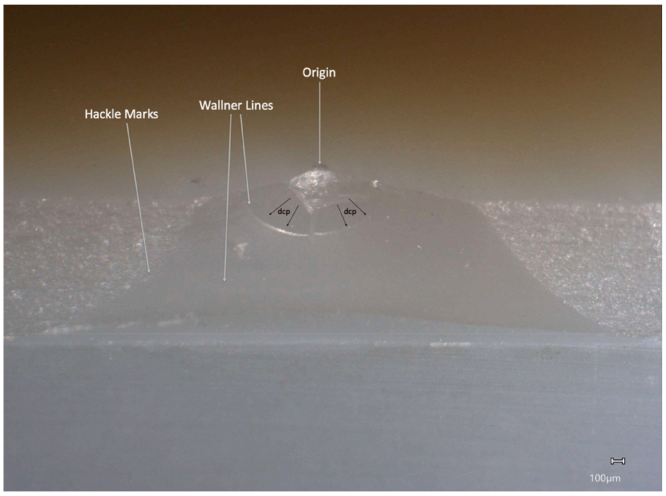

Fig. 5. Overchipping in a fired, hydrothermal-aged CEREC Tessera specimen (1.5 mm thickness, 0.3 mm distance).

ECR ($p < 0.001$). Within 0.3 mm distance, AD-Pol, AD-F and CT-F showed lower ECR than all other groups ($p < 0.001$–0.023), while AM-G&HTF, AM-G&MOF and EC-G&F had higher ECR than all other groups ($p < 0.001$–0.021). Within the hydrothermal-aged groups and 0.25 mm distance, AM-G&MOF showed higher ECR than all other groups ($p < 0.001$–0.013), while AD-F showed lower ECR, than all other groups except CT-F ($p < 0.001$–0.006). Within 0.3 mm distance, AD-Pol and AD-F showed lower ECR, than all other groups except CT-F ($p < 0.001$–0.033).

Fractographic analyses showed that chip geometry increased in size for specimens with higher ECR, while the formation of smaller chips was observed for specimens with lower ECR (Fig. 8).

3.2. Impact of the specimen thickness on ECR

In all aging groups, 3 mm*vs.* 2 mm*thickness*led to higher ECR at 0.25 mm distance for AD-G&F ($p=<0.001$–0.006); 3 mm*vs. 1.*5 mm*thickness*led to higher ECR at 0.3 mm for AD-G&F ($p = 0.007$–0.03).

In non-aged groups, 2 mm*vs. 1.*5 mm*thickness*led to higher ECR at 0.25 mm distance for AD-F ($p = 0.002$) and at 0.3 mm distance for AD-G&F ($p = 0.016$); 1.5 mm*vs.* 2 mm*thickness*led to higher ECR at 0.25 mm distance for AD-G&F ($p = 0.002$); 1.5 mm*vs.* 3 mm*thickness*led to higher ECR at 0.25 mm distance for AM-G&HTF ($p = 0.018$); 2 mm*vs.* 3 mm*thickness*led to higher ECR at 0.25 mm distance for AD-F ($p = 0.034$) and at 0.3 mm distance for CT-F ($p = 0.009$).

In thermal-aged groups, 3 mm *vs.* 2 mm *thickness* led to higher ECR at 0.3 mm distance for AD-G&F, CT-G&F and EC-G&F ($p = 0.004$–0.04); 3 mm *vs. 1.*5 mm *thickness* led to higher ECR at 0.25 mm distance for AD-F ($p = 0.043$), at 0.3 mm distance for CT-F ($p = 0.009$) and at 0.25 mm, as well as at 0.3 mm distance for CT-G&F ($p = 0.01$); 2 mm *vs. 1.*5 mm *thickness* led to higher ECR at 0.25 mm distance for AD-F and CT-G&F ($p = 0.003$–0.004); *1.*5 mm *vs.* 2 mm *thickness* led to higher ECR at 0.25 mm

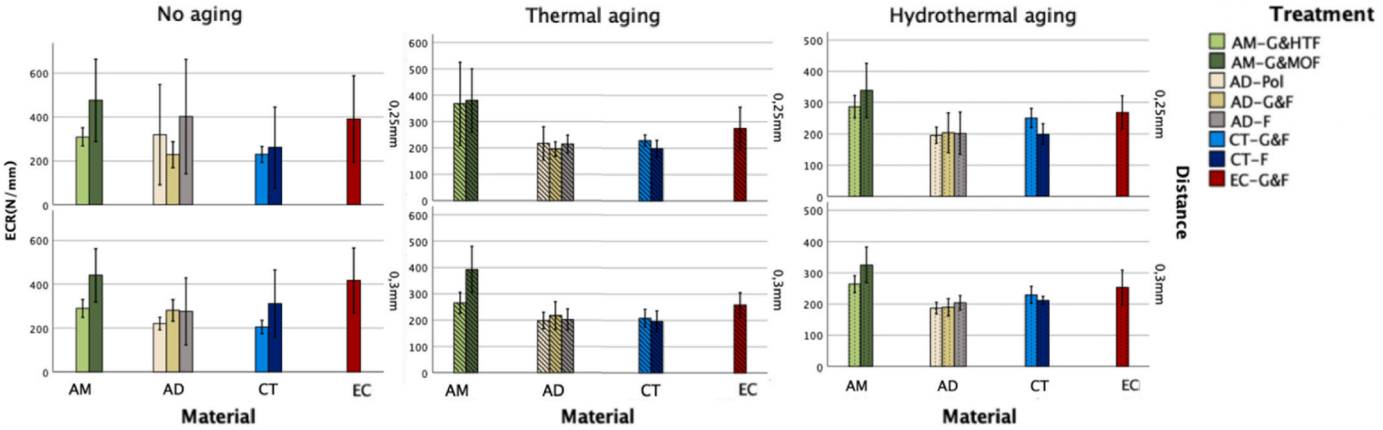

Fig. 6. Edge Chipping results for the four differently treated materials at **2 mm** thickness.

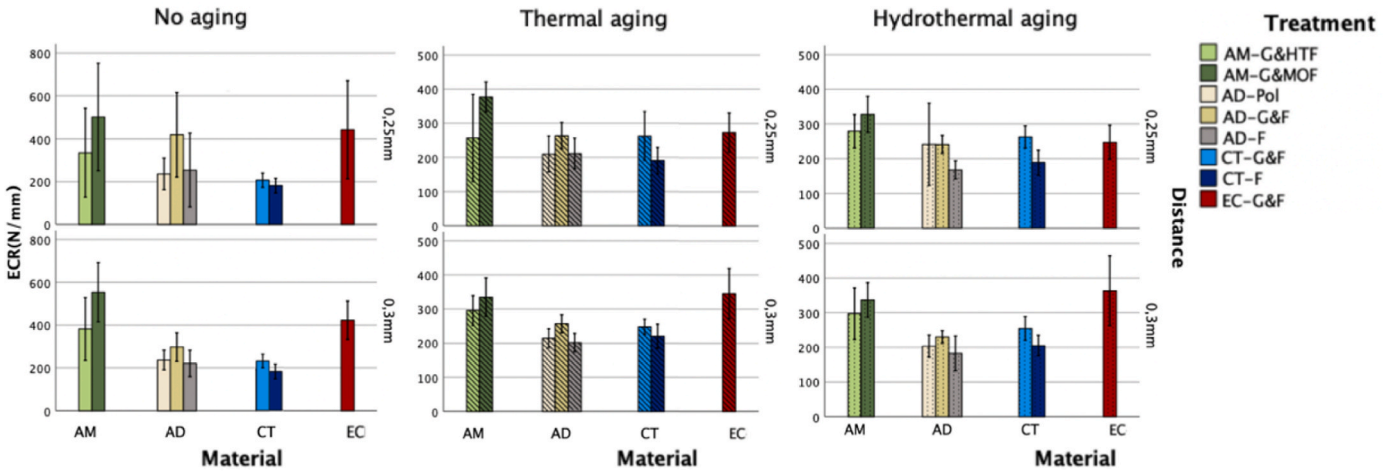

Fig. 7. Edge Chipping results for the four differently treated materials at **3 mm** thickness.

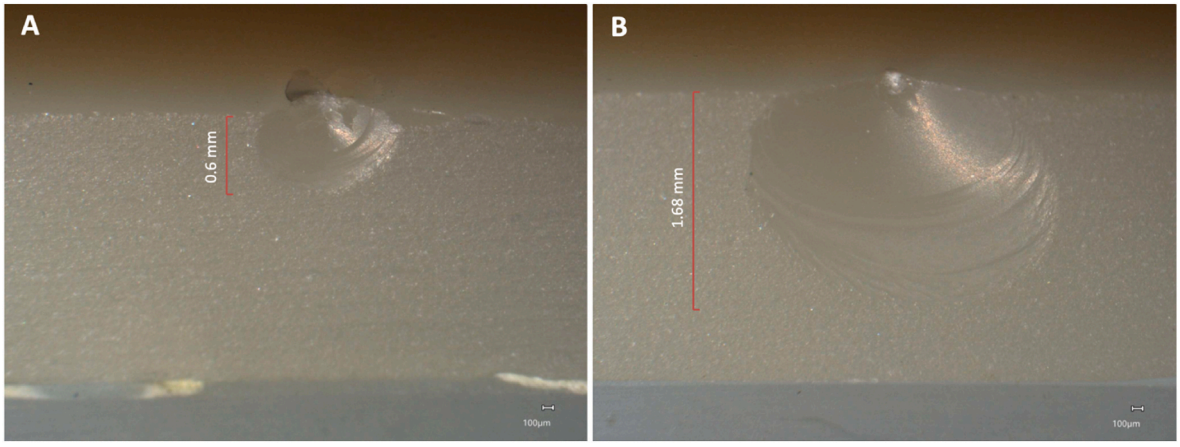

Fig. 8. Higher ECR values correlating with bigger chips. Comparison of 3 mm thick, @0.25 mm distance, hydrothermal-aged Amber Mill Direct specimens either (A) fired or (B) polished.

distance for AD-G&F (p = 0.002) and at 0.3 mm distance for EC-G&F (p = 0.002); *1*.5 mm *vs.* 3 mm *thickness* led to higher ECR at 0.25 mm distance for AM-G&HTF (p = 0.019).

In hydrothermal-aged groups, 3 mm *vs.* 2 mm *thickness* led to higher ECR at 0.3 mm distance for AD-G&F and EC-G&F (p=<0.001–0.011); 3 mm *vs. 1*.5 mm *thickness* led to higher ECR at 0.25 mm distance for AD-G&F and CT-F(p = 0.005–0.019) and at 0.3 mm distance for CT-G&F and EC-G&F (p = 0.044–0.045); 2 mm *vs. 1*.5 mm *thickness* led to higher ECR at 0.25 mm distance for CT-F (p = 0.01).

3.3. Impact of the measuring distance on ECR

A measuring distance of 0.3 mm versus 0.25 mm led to a **higher** ECR for non-aged 2 mm thick AD-G&F (p = 0.015); thermal-aged 3 mm thick AM-G&HTF (p = 0.015), 1.5 mm thick EC-G&F (p = 0.013) and 3 mm thick EC-G&F (p = 0.024) specimens; as well as hydrothermal-aged 3 mm thick EC-G&F specimens (p = 0.006).

A measuring distance of 0.3 mm versus 0.25 mm led to a **lower** ECR for non-aged 1.5 mm thick AD-G&F (p = 0.002); as well as thermal-aged 2 mm thick AM-G&HTF (p = 0.01) and 3 mm thick AM-G&MOF (p = 0.043) specimens.

3.4. Impact of the aging regimen on ECR

Thermal aging led to lower ECR *than no aging* for 1.5 mm & 2 thick at 0.25 mm distance and 3 mm thick at 0.3 mm AM-G&MOF (p = 0.004–0.008), 1.5 mm & 3 mm thick at 0.25 mm distance and 2 mm thick at 0.3 mm distance AD-G&F (p = 0.007–0.034), and 1.5 mm & 3 mm thick at 0.25 mm distance and 2 mm & 3 mm thick at 0.3 mm distance EC-G&F (p = 0.003–0.041).

Hydrothermal aging led to lower ECR *than no aging* for 3 mm thick at 0.3 mm distance AD-F (p = 0.002), and 2 mm & 3 mm thick at 0.3 mm distance and 3 mm thick at 0.25 mm distance EC-G&F (p = 0.005–0.016). Hydrothermal aging led to lower ECR *than no aging or thermal aging* for 1.5 mm thick at 0.3 mm distance and 2 mm thick at 0.25 mm distance AM-G&HTF (p = 0.018–0.041), 1.5 mm thick at 0.25 and 0.3 mm distance and 3 mm thick at 0.3 mm distance AM-G&MOF (p = 0.003–0.008), and 1.5 mm & 3 mm thick at 0.25 mm distance and 2 mm & 3 mm thick at 0.3 mm distance AD-G&F (p = 0.005–0.023). Hydrothermal aging led to higher ECR *than no aging* for 3 mm thick at 0.2 mm distance CT-G&F (p = 0.002).

4. Discussion

The aim of this study was to examine the influence, that different treatment protocols and artificial aging have on the ECR of four lithium silicate ceramics. The null hypotheses, that different lithium silicate ceramics, treatment protocols, specimen thicknesses, measuring distances and aging protocols do not influence the ECR, had to be rejected.

By bonding ceramic specimens to the dentine analogue composite

(GrandioSO x-tra) clinical conditions were approximated, with evidence showing that the bonding of ceramic restorations to underlying substrate, dentine or dentine analogue, lowers failure probability by decreasing the probability of crack initiation (Wang et al., 2006; Burke et al., 2002). Literature investigating the effect of bonding ceramics to a dentine analogue on ECR is scarce, yet evidence suggests that adhesive cementation of the ceramic material to simulated dentine, especially for lower distance from loading point to edge, leads to higher ECR values (Taufer and Della Bona, 2019). GrandioSO x-tra was selected as dentine substitute due to its approximate elastic modulus to dentine, that has been shown to possess values of around 15 GPa (Rees and Jacobsen, 1993; Leprince et al., 2014).

For 7/18 groups (with varying thickness, distance and aging), AM-G&MOF showed higher ECR than all other groups. AM represents a high-performing material with good mechanical properties, especially when fired according to the MOF protocol. While AM-G&HTF overall showed favorable values, firing AM according to the HTF protocol resulted in lower ECR than MOF for 13/18 groups. Hence, MOF is recommended unless an esthetically demanding restoration is to be fabricated in the visible area of the dental arch, where high translucency is of particular esthetical importance (Kelly, 1997). As of today, literature about the esthetic properties of firing AM according to the two different protocols proposed by the manufacturer are lacking, calling for further research to conclusively determine if HTF represents an esthetic advantage.

Within the material AD, a variation in treatment regarding polishing or firing did not lead to changes in ECR for all but one group, whereas G&F led to higher ECR for half of the groups when compared to polishing and higher ECR for 8/18 groups compared to solely firing.

A similar influence of the glazing material can be seen for CT, in which glazed specimens showed a higher ECR than unglazed, fired specimens in more than half of the groups. These findings have implications for the clinical use and long-term durability of restorations made from AD and CT, as the mechanical properties are enhanced through the homogenization of the surface and the glazing materials' migration into initial and propagating microcracks, leading to a strengthening of the ceramic (de Jager et al., 2000; Fairhurst et al., 1992; Emslander et al., 2015). Glazing therefore represents the recommended surface treatment over polishing or solely firing for both AD and CT. These findings are supported by several investigations, that reported enhanced mechanical features of ceramic materials through crystallization or glaze firing compared to surface polishing (Chen et al., 1999; Badawy et al., 2016). Previous investigations have furthermore shown that polishing and glazing influence the surface roughness, translucency parameter, opalescence parameter and contrast ratio of the material and therefore optical properties of the ceramic (Awad et al., 2015; Kurt et al., 2020). In this context, glazing seems to be the preferred method of treatment to provide smooth and esthetic surfaces (Fasbinder and Neiva, 2016). Regarding long-term esthetic results, it has also been shown that glazed lithium-di-silicate specimens were more resistant to discoloration than polished specimens (Saleh et al., 2024). While polishing can help to diminish surface flaws, achieving optimal polishing manually is challenging, as it can be difficult to eradicate all surface defects due to the complex geometry of prosthetic restorations, especially in occlusal areas (Karan and Toroglu, 2008). Then again, polishing is generally more cost-effective than glazing, requiring less specialized equipment, and offers significant time savings as it can be completed more quickly than glazing, which involves initial furnace heating, the application of the glazing material and subsequent firing and cooling times (Sasahara et al., 2006). Depending on the glazing material, furnace and firing protocol and if glazing is done simultaneously to crystallization or separately, the process typically takes around 15–30 min. While these factors highlight the advantages of polishing or exclusive firing of silicate ceramics, particularly in time-sensitive or cost-conscious settings, it must be considered that the mechanical properties of materials pre-treated this way may be inferior to those with glazed surfaces (Mota et al., 2017).

Overall, the lithium-di-silicate ceramics AM and EC showed continuously high ECR values and can be considered suitable materials for clinical use. With AM-G&MOF presenting the overall highest ECR values in 7/18 groups and a higher ECR than EC-G&F in 10/18 groups, the novel material AM shows promising results in comparison with the well-researched EC (Taufer and Della Bona, 2019; Brandeburski and Della Bona, 2020). The more novel composition examined in the lithium-alumina-silicate CT, on the other hand, represented lower ECR values. This may be explained by lithium-alumina-silicate tending to have comparatively low bending strengths and fracture toughness values of around 200 MPa and 1.5 MPa $m^{1/2}$ (Zhang et al., 2018). The properties of lithium-alumina-silicate glass-ceramics are, among other factors, influenced by the ratio of Al^{3+} to Li^{+} ions in their crystallization phases, with mass ratios of Al_2O_3/Li_2O above 5 leading to the material having favorable chemical durability and low thermal expansion, but low mechanical performance (Zhang et al., 2018). Therefore, lithium-alumina-silicate ceramics with mass ratios shifted slightly more towards the proportion of Li_2O exhibit more favorable mechanical properties.

The increased chip sizes in correlation with a higher ECR of the respective material and treatment group may potentially be explained by the fact that materials with a high ECR absorb and dissipate more energy before fracturing, leading to larger chip formations. In contrast, materials with a lower ECR may fracture more easily, resulting in smaller chips due to less energy being absorbed before failure.

The number of groups, where a higher specimen thickness led to a higher ECR, was triple that of groups, where a lower thickness resulted in a higher ECR (24 vs. 8 out of 144 total comparisons). While material thickness did not result in a change of ECR for AD-Pol and had little impact on ECR of AD-F, over half of the AD-G&F treated groups showed higher ECR when specimen thickness was higher. Possibly, the glaze layer in AD-G&F specimens forms a compressive surface layer, that becomes more effective at resisting edge chipping as specimen thickness increases due to an enhanced support from the underlying material. The finding, that the mechanical properties are related to the material thickness, is in line with previous investigations that examined the relation between ceramic thickness and fracture resistance or edge stability (Chen et al., 2014; Pfeilschifter et al., 2018). Restorations with thin margins therefore seem to be at higher risk of fracture or chipping and sufficient material thickness should be considered during tooth preparation and manufacturing to avoid damage or failure of the restoration.

With the high majority of 112/144 comparisons showing no impact of material thickness on ECR and specimens even exhibiting an increased ECR with a reduced material thickness for 8/144 comparisons, a material thickness of 1.5 mm may, however, present limited or no disadvantages compared to a thickness of 2 mm or 3 mm. This finding was evident for AM-G&HTF treated groups, where a reduction of the material thickness either did not influence ECR or – for a smaller proportion of samples – led to higher ECR. A possible explanation for this phenomenon could be that thinner material thicknesses might show different stress distributions, potentially contributing to an increased ECR. This theory could be explained by the finding that tensile stress concentration at the luting surface of the ceramic layer is a predominant factor controlling the failure of ceramic restorations and the observation that a lower ceramic thickness leads to lower stress concentrations at the adhesive interface (Dong and Darvell, 2003; Tribst et al., 2019). Though said findings could lead to the conclusion that through a reduced restoration thickness and minimally invasive preparation design tooth structure could be preserved, these explanations are preliminary and require further investigation to validate their accuracy. Future research should focus on identifying the precise mechanisms leading to increased ECR with decreasing material thicknesses. Detailed analyses of material inhomogeneities, stress distributions, and microstructural properties in thin versus thick samples would be of particular interest.

The measurement distance only had an influence on the ECR in 8/72

groups, contradicting previous findings, that showed a higher ECR with an increased measurement distance (Zadeh et al., 2021; Quinn, 2015). A possible reason for this could be the insufficient difference between the two measurement distances of 0.3 mm and 0.25 mm, which may have been too small to have a measurable impact on ECR. If the variation of the loading point to the restoration margin does, however, not have a significant influence, this finding is of great clinical relevance concerning preparation designs of, for example, inlays. Future research should focus on examining larger variations in measurement distances to investigate the impact of this parameter further.

Specimens underwent artificial aging to simulate temperature fluctuations in the oral cavity, that have been shown to adversely affect the strength of dental restorations and accelerate crack development (Kim et al., 2023). Aging was simulated for 10,000 thermal cycles, corresponding to approximately one year of clinical function, and subsequent hydrothermal aging at 134 °C for a total of 2 h, simulating an additional 6–8 years of in vivo aging (Gale and Darvell, 1999; Morresi et al., 2014). Aging led to a change in ECR for about a third of the groups.

No differences in ECR after aging were found for all distances and thicknesses of AD-Pol and CT-F and only one group of AD-F showed reduced ECR after hydrothermal aging. Previous investigations found a varying impact of thermocycling on the fracture toughness, that has been reported to be directly correlated with ECR of dental silicate ceramics (Kim et al., 2023; Fouda et al., 2024). One investigation found no decline in fracture toughness after thermal aging, supposedly explained by the high crystalline content in silicate ceramics and therefore increased hardness and elastic modulus, making the material more resistant to the damaging effects of thermal changes compared to hybrid materials like resin nanoceramics (Kim et al., 2023; Fouda et al., 2024). For groups unaffected by artificial aging, this indicates that the properties of these specifically treated groups are stable enough not to be noticeably affected by the aging process or that the duration or conditions of aging were not sufficient to induce significant changes.

Aging led to reduced ECR values for 15/30 a.m.-G&HTF, AM-G&MOF, AD-G&F and EC-G&F groups. Research has shown a reduced flexural strength of silicate ceramics following fatigue protocols, reasoning that thermal shocks and rapid cooling of ceramic surfaces can induce tensile stress, weakening the material, causing micro-crack formation and subsequent penetration of water (de Pinho Barcellos et al., 2018; Quinn, 2016; Shafter et al., 2017). In this investigation, changes in ECR after artificial aging were exclusively observed in groups that received glazing. The glaze layer might be susceptible to wear, development of surface flaws and chemical degradation through thermal fluctuations over time, diminishing its protective effect and leading to decreased ECR. While ceramics, including ceramic glazing masses, are considered minimally soluble (Sagsoz and Polat Sagsoz, 2019), previous investigations have shown chemical degradation of ceramics attributed to mechanical and chemical environmental factors (Elshahawy et al., 2013; Milleding et al., 2002). The wear and degradation process may be less pronounced in polished or solely fired specimens, which do not have the additional, more vulnerable layer. Interestingly, CT-G&F displayed increased ECR values after combined thermal and hydrothermal treatment for one out of six groups, warranting further investigations. For clinical handling it can be stated that, although the glazed groups exhibited changes or a decline in ECR after artificial aging, ECR values for glazed groups were still higher than those of the groups subjected to other surface treatments and discouraging the use of glaze masses compared to solely firing or polishing is not recommended. However, it is essential to investigate whether the observed decrease in ECR continues with prolonged aging to make long-term predictions and recommendations regarding the use of glazing in ceramic restorations.

Limitations of this investigation include that the shape of the chipping fractures was not consistent across all specimens, with some groups showing overchipping, leading to a reduced number of measurements or none for the affected groups. Additionally, the in-vitro set-up must as well be stated as limiting and the flat-layer configurations of the specimens examined oversimplify the geometries of actual dental restorations. In clinical reality, critical loads for chipping at increased distances from the side walls have proven to be lower on the curved surfaces of anatomically shaped crowns compared to specimens with flat geometry (Zhang et al., 2013). With preliminary tests not showing a difference between incisal and occlusal ECR measurement ($p = 0.712$), the strength gradient of AD indicated by the manufacturer was not considered during measurements. Future studies investigating this property are called for.

5. Conclusion

The conducted investigation highlights the impact of varying surface treatments, restoration thicknesses, the point of loading and aging of lithium silicate ceramics on their edge chipping behavior. Within the limitations of this investigation, the following conclusions can be drawn: Out of all groups, AM-G&MOF exhibited the most favorable ECR behavior, surpassing the tried and tested EC-G&F. In groups where specimens of the same ceramic material underwent varying surface treatments such as polishing, glazing & firing or exclusive firing, glazed specimens demonstrated a higher ECR. With a high majority of groups showing no impact of the specimen thickness on the ECR, a reduced restoration thickness of 1.5 mm seems to present limited disadvantages compared to 2 mm or 3 mm. No clear trend could be observed regarding a change in ECR in dependence of the distance from the point of loading to the specimen's edge. Though artificial aging led to a reduction in ECR in some glazed groups, their ECR values remained comparatively high, underlining that glazing can be recommended as the preferred method of surface treatment.

CRediT authorship contribution statement

Carola Irlinger: Writing – original draft, Visualization, Investigation, Formal analysis, Data curation. **Bogna Stawarczyk:** Writing – review & editing, Supervision, Resources, Project administration, Methodology, Formal analysis, Conceptualization. **John Meinen:** Writing – review & editing, Resources, Methodology. **Daniel Edelhoff:** Writing – review & editing, Validation, Supervision, Resources, Conceptualization. **Felicitas Mayinger:** Writing – review & editing, Supervision, Resources, Methodology, Data curation, Conceptualization.

Declaration of competing interest

The authors declare that they have no known competing financial interests or personal relationships that could have appeared to influence the work reported in this paper.

Acknowledgements

The authors would like to thank Dentsply Sirona, HASS Cooperation, Ivoclar and VOCO for supporting this study with the respective materials.

Data availability

Data will be made available on request.

References

Alao, A.R., Stoll, R., Zhang, Y., Yin, L., 2021. Influence of CAD/CAM milling, sintering and surface treatments on the fatigue behavior of lithium disilicate glass ceramic. J. Mech. Behav. Biomed. Mater. 113, 104133.
Anusavice, K.J., 1992. Degradability of dental ceramics. Adv. Dent. Res. 6, 82–89.
Asai, T., Kazama, R., Fukushima, M., Okiji, T., 2010. Effect of overglazed and polished surface finishes on the compressive fracture strength of machinable ceramic materials. Dent. Mater. J. 29, 661–667.

Awad, D., Stawarczyk, B., Liebermann, A., Ilie, N., 2015. Translucency of esthetic dental restorative CAD/CAM materials and composite resins with respect to thickness and surface roughness. J. Prosthet. Dent 113, 534–540.
Badawy, R., El-Mowafy, O., Tam, L.E., 2016. Fracture toughness of chairside CAD/CAM materials - alternative loading approach for compact tension test. Dent. Mater. 32, 847–852.
Brandeburski, S.B.N., Della Bona, A., 2020. Quantitative and qualitative analyses of ceramic chipping. J. Mech. Behav. Biomed. Mater. 110, 103928.
Burke, F.J., Fleming, G.J., Nathanson, D., Marquis, P.M., 2002. Are adhesive technologies needed to support ceramics? An assessment of the current evidence. J. Adhesive Dent. 4, 7–22.
Chen, H.Y., Hickel, R., Setcos, J.C., Kunzelmann, K.H., 1999. Effects of surface finish and fatigue testing on the fracture strength of CAD-CAM and pressed-ceramic crowns. J. Prosthet. Dent 82, 468–475.
Chen, C., Trindade, F.Z., de Jager, N., Kleverlaan, C.J., Feilzer, A.J., 2014. The fracture resistance of a CAD/CAM resin nano ceramic (RNC) and a CAD ceramic at different thicknesses. Dent. Mater. 30, 954–962.
Coldea, A., Fischer, J., Swain, M.V., Thiel, N., 2015. Damage tolerance of indirect restorative materials (including PICN) after simulated bur adjustments. Dent. Mater. 31, 684–694.
de Jager, N., Feilzer, A.J., Davidson, C.L., 2000. The influence of surface roughness on porcelain strength. Dent. Mater. 16, 381–388.
de Pinho Barcellos, A.S., Marinho, C.C., Miranda, J.S., Amaral, M., Shiino, M.Y., Kimpara, E.T., 2018. Effect of fatigue protocols on flexural strength of lithium disilicate bars with clamped-ends. J. Mech. Behav. Biomed. Mater. 81, 173–177.
Denry, I., 2013. How and when does fabrication damage adversely affect the clinical performance of ceramic restorations? Dent. Mater. 29, 85–96.
Deville, S., Chevalier, J., Gremillard, L., 2006. Influence of surface finish and residual stresses on the ageing sensitivity of biomedical grade zirconia. Biomaterials 27, 2186–2192.
Dong, X.D., Darvell, B.W., 2003. Stress distribution and failure mode of dental ceramic structures under Hertzian indentation. Dent. Mater. 19, 542–551.
Elshahawy, W., Ajlouni, R., James, W., Abdellatif, H., Watanabe, I., 2013. Elemental ion release from fixed restorative materials into patient saliva. J. Oral Rehabil. 40, 381–388.
Emslander, A., Reise, M., Eichberger, M., Uhrenbacher, J., Edelhoff, D., Stawarczyk, B., 2015. Impact of surface treatment of different reinforced glass-ceramic anterior crowns on load bearing capacity. Dent. Mater. J. 34, 595–604.
Fairhurst, C.W., Lockwood, P.E., Ringle, R.D., Thompson, W.O., 1992. The effect of glaze on porcelain strength. Dent. Mater. 8, 203–207.
Fasbinder, D.J., Neiva, G.F., 2016. Surface evaluation of polishing techniques for new resilient CAD/CAM restorative materials. J. Esthetic Restor. Dent. 28, 56–66.
Fouda, A.M., Bourauel, C., Samran, A., Kassem, A.S., Alhotan, A., 2024. Effect of glazing and thermocycling on the fracture toughness and hardness of a new fully crystallized aluminosilicate CAD/CAM ceramic material. BMC Oral Health 24, 620.
Freitas, J.S., Souza, L.F.B., Dellazzana, F.Z., Silva, T., Ribeiro, L., Pereira, G.K.R., et al., 2023. Advanced lithium disilicate: a comparative evaluation of translucency and fatigue failure load to other ceramics for monolithic restorations. J. Mech. Behav. Biomed. Mater. 148, 106192.
Gale, M.S., Darvell, B.W., 1999. Thermal cycling procedures for laboratory testing of dental restorations. J. Dent. 27, 89–99.
Joshi, G.V., Duan, Y., Della Bona, A., Hill, T.J., St John, K., Griggs, J.A., 2014. Contributions of stress corrosion and cyclic fatigue to subcritical crack growth in a dental glass-ceramic. Dent. Mater. 30, 884–890.
Karan, S., Toroglu, M.S., 2008. Porcelain refinishing with two different polishing systems after orthodontic debonding. Angle Orthod. 78, 947–953.
Kelly, J.R., 1997. Ceramics in restorative and prosthetic dentistry. Annu. Rev. Mater. Res. 27, 443–468.
Kim, S.Y., Bae, H.J., Lee, H.H., Lee, J.H., Kim, Y.J., Choi, Y.S., et al., 2023. The effects of thermocycling on the physical properties and biocompatibilities of various CAD/CAM restorative materials. Pharmaceutics 15.
Kurt, M., Bankoğlu Güngör, M., Karakoca Nemli, S., Turhan Bal, B., 2020. Effects of glazing methods on the optical and surface properties of silicate ceramics. J Prosthodont Res 64, 202–209.
Leprince, J.G., Palin, W.M., Vanacker, J., Sabbagh, J., Devaux, J., Leloup, G., 2014. Physico-mechanical characteristics of commercially available bulk-fill composites. J. Dent. 42, 993–1000.
Li, M., Dong, C., Ma, Y., Jiang, H., 2023. Light-transmitting lithium aluminosilicate glass-ceramics with excellent mechanical properties based on cluster model design. Nanomaterials 13, 530.
Lohbauer, U., Fabris, D.C.N., Lubauer, J., Abdelmaseh, S., Cicconi, M.-R., Hurle, K., et al., 2024. Glass science behind lithium silicate glass-ceramics. Dent. Mater. 40, 842–857.
Lu, Y., de Oliveira Dal Piva, A.M., Tribst, J.P.M., Feilzer, A.J., Kleverlaan, C.J., 2023. Does glaze firing affect the strength of advanced lithium disilicate after simulated defects? Clin. Oral Invest. 27, 6429–6438.
Milleding, P., Haraldsson, C., Karlsson, S., 2002. Ion leaching from dental ceramics during static in vitro corrosion testing. J. Biomed. Mater. Res. 61, 541–550.
Mores, R.T., Borba, M., Corazza, P.H., Della Bona, Á., Benetti, P., 2017. Influence of surface finishing on fracture load and failure mode of glass ceramic crowns. J. Prosthet. Dent 118, 511–516.
Morresi, A.L., D'Amario, M., Capogreco, M., Gatto, R., Marzo, G., D'Arcangelo, C., et al., 2014. Thermal cycling for restorative materials: does a standardized protocol exist in laboratory testing? A literature review. J. Mech. Behav. Biomed. Mater. 29, 295–308.
Mota, E.G., Smidt, L.N., Fracasso, L.M., Burnett, Jr.LH., Spohr, A.M., 2017. The effect of milling and postmilling procedures on the surface roughness of CAD/CAM materials. J. Esthetic Restor. Dent. 29, 450–458.
Pfeilschifter, M., Preis, V., Behr, M., Rosentritt, M., 2018. Edge strength of CAD/CAM materials. J. Dent. 74, 95–100.
Quinn, G.D., 2015. On edge chipping testing and some personal perspectives on the state of the art of mechanical testing. Dent. Mater. 31, 26–36.
Quinn, G., 2016. Fractography of Ceramics and Glasses, second ed. U.S. Government, National Institute of Standards and Technology, Gaithersburg, MD.
Quinn, G.D., Giuseppetti, A.A., Hoffman, K.H., 2014. Chipping fracture resistance of dental CAD/CAM restorative materials: part I–procedures and results. Dent. Mater. 30, e99–e111.
Rees, J.S., Jacobsen, P.H., 1993. The elastic moduli of enamel and dentine. Clin. Mater. 14, 35–39.
Rosentritt, M., Schmid, A., Huber, C., Strasser, T., 2022. In vitro mastication simulation and wear test of virgilite and advanced lithium disilicate ceramics. Int. J. Prosthodont. (IJP) 35, 770–776.
Sagsoz, O., Polat Sagsoz, N., 2019. Chemical degradation of dental CAD/CAM materials. Bio Med. Mater. Eng. 30, 419–426.
Saleh, K.A.E.-D., Hammad, I.A., Aly, Y.M., 2024. Color stability of glazed and polished lithium disilicate PRESSABLE glass ceramic after immersion in mouth rinses: an in vitro study. Alexandria Dental Journal 49, 148–152.
Salmang, H., Scholze, H., 2007. Keramik, seventh ed. Springer, Berlin/Heidelberg, Germany.
Sasahara, R.M., Ribeiro Fda, C., Cesar, P.F., Yoshimura, H.N., 2006. Influence of the finishing technique on surface roughness of dental porcelains with different microstructures. Operat. Dent. 31, 577–583.
Shafter, M., Jain, V., Wicks, R., Nathanson, D., 2017. Effect of thermocycling on flexural strength of different CAD/CAM material. Journal of Dentistry & Oral Disorders 3.
Stawarczyk, B., Mandl, A., Liebermann, A., 2021. Modern CAD/CAM silicate ceramics, their translucency level and impact of hydrothermal aging on translucency, martens hardness, biaxial flexural strength and their reliability. J. Mech. Behav. Biomed. Mater. 118, 104456.
Taufer, C., Della Bona, A., 2019. Edge chipping resistance of ceramics bonded to a dentine analogue. J. Mech. Behav. Biomed. Mater. 90, 587–590.
Tribst, J.P., Kohn, B.M., de Oliveira Dal Piva, A.M., Spinola, M.S., Borges, A.L., Andreatta Filho, O.D., 2019. Influence of restoration thickness on the stress distribution of ultrathin ceramic onlay rehabilitating canine guidance: a 3D-finite element analysis. Minerva Stomatol. 68, 126–131.
Wang, R., Katsube, N., Seghi, R., Rokhlin, S., 2006. Statistical failure analysis of brittle coatings by spherical indentation: theory and experiment. J. Mater. Sci. 41, 5441–5454.
Zadeh, P.N., Stawarczyk, B., Hampe, R., Liebermann, A., Mayinger, F., 2021. Edge chipping resistance of veneering composite resins. J. Mech. Behav. Biomed. Mater. 116, 104349.
Zhang, Y., Kelly, J.R., 2017. Dental ceramics for restoration and metal veneering. Dent. Clin. 61, 797–819.
Zhang, Y., Kim, J.W., Bhowmick, S., Thompson, V.P., Rekow, E.D., 2009. Competition of fracture mechanisms in monolithic dental ceramics: flat model systems. J. Biomed. Mater. Res. B Appl. Biomater. 88, 402–411.
Zhang, Y., Lee, J.J., Srikanth, R., Lawn, B.R., 2013. Edge chipping and flexural resistance of monolithic ceramics. Dent. Mater. 29, 1201–1208.
Zhang, Y., Guo, H., Zhang, H., Deng, Y., Wang, B., Yang, J., 2018. Effect of added mullite whisker on properties of lithium aluminosilicate (LAS) glass-ceramics prepared for dental restoration. J. Biomed. Nanotechnol. 14, 1944–1952.